

# SPINNING-UP THE ENVELOPE BEFORE ENTERING A COMMON ENVELOPE PHASE

Ealeal Bear<sup>1</sup> and Noam Soker<sup>1</sup>

## ABSTRACT

We calculate the orbital evolution of binary systems where the primary star is an evolved red giant branch (RGB) star, while the secondary star is a low mass main sequence (MS) star or a brown dwarf. The evolution starts when a tidal interaction causes the secondary to spiral-in. Either a common envelope (CE) is formed in a very short time, or the system reaches synchronization and the spiraling-in process substantially slows down. Some of these systems later enter a CE phase. We find that for a large parameters space, binary systems reach stable synchronized orbit before the onset of a CE phase. Such stable synchronized orbits allow the RGB star to lose mass prior to the onset of the CE phase. Even after the secondary enters the giant envelope, the rotation velocity is high enough to cause enhanced mass loss rate. Our results imply that it is crucial to include the pre-CE evolution when studying the outcome of the CE phase. Although we have made the calculations for RGB stars, the results have implications for other evolved stars that interact with close companions.

## 1. Introduction

Extreme horizontal branch (EHB) stars are post red giant branch (RGB) stars that burn helium in their core and have a very low mass envelope. Spectroscopically they are classified as sdB (or sdO) stars, although some sdB and sdO stars might be post asymptotic giant branch (AGB) stars. In what follows we will refer by sdB stars only to EHB stars, and sdB include sdO stars as well. Many of the sdB stars in the field (i.e., not in globular clusters) are in binary systems (Maxted et al. 2001a,b), some with a close and very faint M type main sequence (MS) companion, e.g., HS 0705 + 6700 (Drechsel et al 2001), PG 1336 – 018 (Kilkenny et al. 1998), and HW Vir (Menzies & Marang 1986; Wood et al. 1993).

The orbital and physical parameters of the three systems HS 0705 + 6700, PG 1336 – 018, and HW Vir, are very similar (Drechsel et al 2001). In HS 0705 + 6700, for example, the sdB

---

<sup>1</sup>Department of Physics, Technion–Israel Institute of Technology, Haifa 32000 Israel; ealealbh@gmail.com; soker@physics.technion.ac.il.

and secondary stellar masses and radii are  $M_1 = 0.483M_\odot$ ,  $M_2 = 0.134M_\odot$ ,  $R_1 = 0.230R_\odot$ , and  $R_2 = 0.186R_\odot$ , respectively, while the orbital separation and period are  $0.81R_\odot$ , and  $2^{\text{h}}18^{\text{m}}$ , respectively. It turns out that the secondary star almost fills its roche lobe (Drechsel et al 2001). Typically these systems have  $q \equiv M_2/M_1 \lesssim 0.3$ . Detection is biased toward close and more massive companions. This suggests that many more systems exist with even lower values of  $q$  (Davis et al. 2009). Geier et al. (2009), for example, announced recently the detection of a  $8 - 23M_J$ , where  $M_J$  is Jupiter mass, substellar companion orbiting an sdB star at an orbital separation of  $5 - 6.1R_\odot$ .

These systems must have gone through a common envelope (CE) phase (e.g., Livio & Soker 1988; Drechsel et al. 2001; Han et al. 2007 and Han 2008 for recent papers with more references). Different aspects regarding the formation of sdB stars and the evolution of RGB stars through a CE phase have been discussed in the literature for more than three decades (e.g., Pustynski & Pustynnik 2006; Soker 2006; Livio & Soker 2002; Dewi & Tauris 2000; D’Cruz et al 1996; Alexander 1976; Paczynski 1971; Han et al. 2002, 2003, 2007; Han 2008). However, some questions remain open. (1) Does the companion transfer part, or all, of the mass it accreted during the CE phase back to the primary at the end of the CE phase? (2) What is the role played by very low mass MS companions, considering that even substellar objects (brown dwarfs and planets) can form sdB stars, as suggested by one of us in a series of papers (Soker 1998, Soker & Harpaz 2000, 2007), and confirmed observationally by Geier et al. (2009)?

In the present paper we examine how tidal interaction before the formation of the CE might increase the likelihood of a low mass MS companion to survive the CE phase. In section 2 we explain the basic mechanism and present simple solutions ignoring the evolution of the primary star along the RGB (but mass loss is included). In section 3 we also consider the increase in the stellar core mass and stellar radius. We summarize our main results in section 4.

## 2. Basic characteristics of the evolution

The onset of the CE, and the ejection of the envelope before and after the onset of the CE, have received a great deal of attention over the years (e.g., Soker et al 1984; Tauris & Dewi 2001; Han et al. 2002; De Marco et al. 2003; Soker 2004; Hu et al. 2007; Nelemans & Tout 2005; Beer et al. 2007; Politano & Weiler 2007; Webbink 2008; Davis et al. 2009). Our goal is to study in more detail the evolution of binary systems in a stage prior to the onset of the CE phase, and in particular systems that have reached synchronization; the synchronization is between the orbital period and the primary rotation period.

We start our calculation when tidal interaction becomes important. For the binary systems we study, where the primary is an RGB star and the secondary is a low mass main sequence (MS) star or a brown dwarf, tidal interaction becomes important when the giant swells to a radius of  $R_g \sim 0.2a$ , where  $a$  is the orbital separation (Soker 1998). The primary radius increases along the RGB as the core mass increases. The primary and the secondary initial masses ranges in the binary

systems we study are  $0.8M_{\odot} \leq M_1 \leq 2.2M_{\odot}$ , and  $0.015M_{\odot} \leq M_2 \leq 0.2M_{\odot}$ , respectively.

As a binary system starts its evolution it is not synchronized, and therefore tidal interaction will lead to a fast spiraling-in process, i.e., the orbital separation decreases. The binary system can then either reach a synchronization or stays asynchronous. In the asynchronous systems tidal interaction will lead to a fast spiraling-in process all the way to a rapid formation of a CE. In systems where synchronization is reached the orbital evolution substantially slows down (unless a Darwin instability occurs as soon as synchronization is achieved; see below), as its rate is now controlled by mass loss and the evolution of the primary star; the orbital separation can decrease or increase.

When orbital separation increases faster than the RGB stellar radius, the evolution is terminated when all the primary envelope is lost, or a core helium flash occurs; no CE phase occurs. If the orbital separation decreases relative to the RGB stellar radius, the evolution ends when at least one of the following conditions occur:

- (1) When the mass of the primary envelope has been totally lost. No CE phase occurs.
  - (2) When the core experiences a core helium flash. Here we take this to occur when the core mass reaches  $0.48M_{\odot}$ . No CE phase occurs.
  - (3) Darwin Instability (see below) is reached, the secondary falls into the primary envelope.
  - (4) The RGB stellar radius increases to the point where it engulfs the secondary, namely,  $R_g > a$ .
- If conditions (3) or (4) are met, the system enters a CE phase after some fraction, even a large fraction, of the primary envelope has been lost.

The different types of behavior are presented in Fig. 1. This figure includes the evolution of the primary star, and the detail of the calculation will be presented in section 3. Here we are only interested in the general outcome. The orbital separation (in units of  $R_{\odot}$ ) versus time is presented for several cases, as indicated in the figure. When the secondary mass is too low (exact value depends on the RGB stellar properties) the secondary star does not have enough orbital angular momentum to bring the primary rotation to be synchronized with the orbital period. Tidal interaction rapidly cause the secondary to spiral-in and form a CE. We do not calculate the tidal time scale, as it is very short.

When the secondary mass is larger than some critical value for the same RGB star, a synchronization is achieved (in a short time) before the orbital separation decrease to the RGB radius. (As we do not treat the initial process of reaching synchronization, the calculation seems to start from a radius of smaller that the primordial orbital separation.) Now the system evolves on a mass loss time scale. The primary star loses mass, an effect that tends to increase orbital separation. However, the wind carries angular momentum. To maintain synchronization the secondary transfers, via tidal forces, orbital angular momentum to the envelope, and the orbit shrinks. Tidal effect might overcomes the mass loss effect. Eventually, a point is reached where the secondary enters the envelope, either due to the Darwin instability, or by the swelling RGB envelope that increases to  $R_g = a$ . By that time the envelope mass is lower than its initial value. Calculations that do not

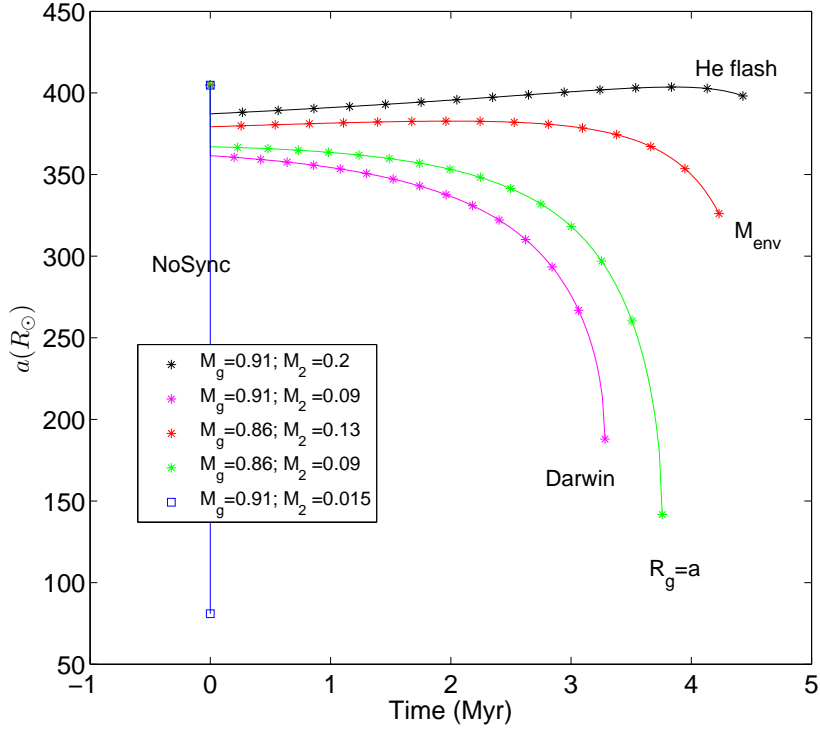


Fig. 1.— Orbital separation, in solar radii for different binaries as indicated, vs. time. The termination of the evolution is indicated. NoSync: No stable synchronized orbit is reached, and a rapid CE phase occurs;  $M_{\text{env}}$ : the RGB has lost its envelope;  $R_g = a$ : the RGB stellar radii increased to the point it swallowed the secondary; Darwin: the Darwin instability caused the formation of a common envelope; He flash: the core mass reached a mass of  $0.48M_{\odot}$  and a He core flash was assumed. The initial RGB stellar mass  $M_g$  and secondary mass  $M_2$  for each case are indicated in the legend. In all cases the mass loss parameter in equation (8) is  $\eta_R = 3 \times 10^{-13}$ , the initial core mass is  $M_c(0) = 0.4M_{\odot}$ , the orbital separation prior to tidal interaction is  $a_0 = 5R_g(0) = 405R_{\odot}$ , and the calculations include the primary evolution as explained in section 3.

consider the possibility of pre-CE mass loss might attribute the entire mass loss to the CE phase. Such calculations overestimate the efficiency by which the secondary expels the envelope during the CE phase. This overestimate can lead to a search for an extra energy source that is actually not required.

When the secondary mass is larger even (for the same RGB star), the secondary orbit shrinks by a small amount before it brings the primary to synchronization. As the orbital separation is large, the effect of mass loss overcomes the effect of angular momentum transfer by tidal interaction and the orbital separation increases.

To demonstrate the basic characteristics of the evolution, we start by neglecting the evolution of the RGB star. Namely, we assume the core mass and RGB stellar radius to be constant, as in Soker (2002). As a single star reaches this radius its rotation angular velocity  $\omega$  will be very small; practically zero. When synchronization is achieved, it is done on a short time, and we neglect angular momentum loss in the wind, such that the source of most of the RGB angular momentum  $J_{\text{env}} = I_{\text{env}}\omega$ , is the change in the orbital angular momentum  $\Delta J_{\text{orb}}$ , where  $I_{\text{env}}$  is the envelope's moment of inertia. Namely,

$$I_{\text{env}}\omega_{\text{syn}} = \Delta J_{\text{orb}}, \quad (1)$$

where  $\omega_{\text{syn}}$  is the angular velocity of the primary envelope when synchronization is achieved for the first time, and

$$\Delta J_{\text{orb}} = \mu(GM)^{0.5} (a_0^{0.5} - a_{\text{syn}}^{0.5}), \quad (2)$$

where  $a_0$  is the orbital separation prior to synchronization (when tidal interaction becomes important), and is set here to  $a_0 = 5R_g(0)$ , and  $a_{\text{syn}}$  is the orbital separation when synchronization is achieved for the first time. As usual,  $M \equiv M_g + M_2$  and  $\mu \equiv M_g M_2 / M$ . Synchronization implies the equality

$$\omega_{\text{syn}} = [GM_g(a_{\text{syn}})^{-3}]^{0.5}, \quad (3)$$

for  $M_2 \ll M_g$ .

Due to its small size, the core's angular momentum is negligible. The angular momentum carried by the wind must be considered after synchronization is achieved because the evolution slows down, and the primary's mass loss rate on the RGB is significant over a long time. Actually, under the assumption that the primary core does not evolve, the evolution is controlled by mass loss. Conservation of angular momentum determines the evolution

$$\dot{J}_{\text{orb}} + \dot{J}_{\text{env}} + \dot{J}_{\text{wind}} = 0. \quad (4)$$

Using the evaluation of equation (4) as given by Soker (2002), we solved for the orbital evolution as function of mass loss for an RGB star with constant core mass of  $M_c = 0.4M_\odot$  and radius of  $R_g(0) = 81R_\odot$ . Tidal interaction is assumed to start when the stellar radius grows to  $R_g = 0.2a_0$ , hence here we set  $a_0 = 5R_g(0) = 405R_\odot$ , and a constant core mass of  $M_c = 0.4M_\odot$  (for details see Soker 2002). The RGB radius is fixed at  $R_g(0) = 81R_\odot$ . When the evolution of the primary is

not considered, the orbital separation is a function of the envelope mass. For that case there is an analytical solution to determined if a stable synchronization orbit is achieved.

In some cases when synchronization is achieved, the system is already unstable to the Darwin instability. This instability sets in when a small decrease in the orbital radius does not transfer enough angular momentum to the spinning primary to maintain a synchronization. The condition for stability is  $I_{\text{orb}} > 3I_{\text{env}}$ , where  $I_{\text{orb}} = M_g M_2 / (M_g + M_2) a^2$  is the orbital moment of inertia, and  $I_{\text{env}} = \eta M_{\text{env}} R_g^2$  for the envelope's moment of inertia. For RGB stars  $\eta \simeq 0.2$ . Taking again  $M_2 \ll M_g$ , the instability sets in when

$$M_2 a^2 = 3\eta M_{\text{env}} R_g^2. \quad (5)$$

Equations (1), (2), (3) and (5) can be combined to yield the condition that a stable synchronized orbit is achieved, that for  $M_2 \ll M_g$  can be approximated as

$$M_2 > \frac{4^4 \eta}{3^3} \left( \frac{a_0}{R_g} \right)^{-2} M_{\text{env}}. \quad (6)$$

Taking  $a_0 = 5R_g$  as before,  $\eta = 0.2$ , and  $M_{\text{env}} = M_g - 0.4$ , for a core mass of  $M_c = 0.4M_\odot$  (masses in solar units if not indicated otherwise), in equation (6) gives

$$M_2 > 0.076 M_{\text{env}} = 0.076 (M_g - 0.4 M_\odot). \quad (7)$$

This represents a straight line in the  $M_g - M_2$  plane, drawn as straight blue line in Fig. 2.

In Fig. 2 we present by a wide strip the region in the  $M_g - M_2$  plane where the systems reach synchronization before the onset of a CE. Above this strip the companion spiral-in to the envelope before a synchronization is achieved. Below that strip, the secondary avoids the CE. As found already by Soker (2002), this strip is very narrow. The line according to equation (7) is also drawn on the figure, just on the upper-left boarder of the strip. To better explore the possibility of significant mass loss prior to the onset of a common envelope, we turn to include the primary evolution. 3.

### 3. Calculations with an evolving primary star

#### 3.1. Basic equations

When the evolution of the primary is not considered, the orbital separation is a function solely of the envelope mass, as the core mass and radius are constant. In that case the dependence on time comes from the mass loss rate. In this section the increase in core mass and its influence on the primary RGB star are taken into considerations. The mass loss from the envelope is calculated

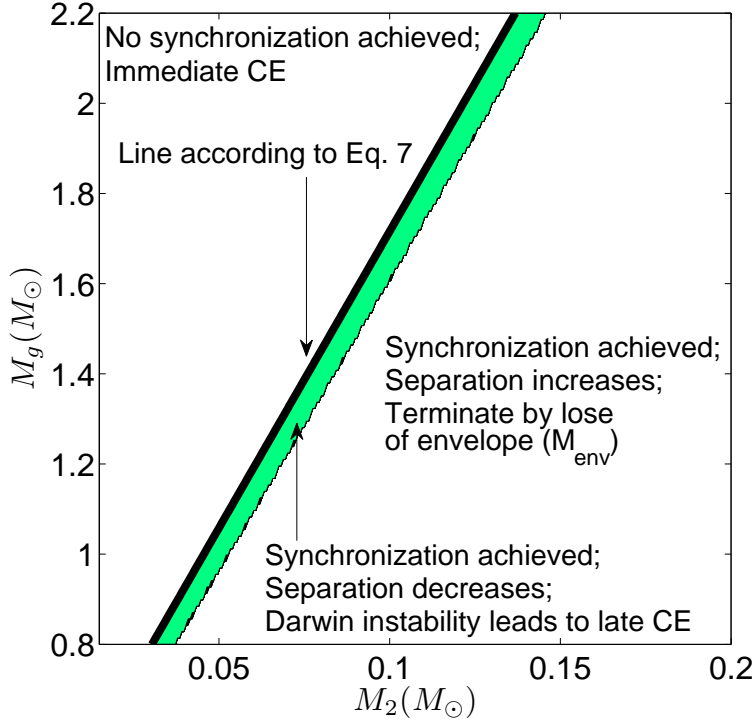


Fig. 2.—  $M_g$  vs.  $M_2$  for binaries with a constant RGB core mass  $M_c$ , and hence constant radius  $R_g$  (RGB evolution is not considered). The upper-left trapeze represents binaries that did not achieve synchronization, but rather formed an immediate CE. The lower-right trapeze represents binaries that achieved synchronization, but never formed a CE. In these cases the envelope was depleted, mainly due to the RGB wind. The thick strip in the  $M_2/M_g$  plane is for binaries that achieved synchronization before they entered a late CE. The straight line represents equation (7). In all cases here the mass loss parameter in equation (8) is  $\eta_R = 3 \times 10^{-13}$ , the core mass is  $M_c = 0.4M_\odot$ , and the orbital separation prior to onset of tidal interaction (primordial separation) is  $a_0 = 5R_g(0) = 405R_\odot$ .

by the Reimers equation (Reimers 1975; see, e.g., Catelan 2009, Schoder & Cuntz 2007, Suzuki 2007, and Meszaros et al. 2009 for recent usages and discussions of that formula)

$$\dot{M}_g = \eta_R L_\odot R_\odot / M_\odot \quad (8)$$

Although this formula is commonly used to estimate the mass loss from the giant, most researchers agree that it does not cover all the physical mechanism and characteristics. For example, we know from the different distribution of HB stars in different globular clusters that other effects, such as metallicity, influences the wind ejection process (e.g., D’Cruz et al 1996, 2000; Whitney et al. 1998; Catelan 2000). The value of  $\eta_R$  has been discussed in length in the literature. Since it was shown that the Reimers formula underestimates the wind ejected from some giants (Schroder & Kuntz 2005, Suzuki 2007), we will explore the results for two values:  $\eta_R = 3 \times 10^{-14}$  (normal), and  $\eta_R = 3 \times 10^{-13}$  (high).

In this section we consider the nuclear evolution of the star. Nuclear burning increases the core mass, implying increase in luminosity and RGB radius. For the growth rate of the RGB core we take an expression given by Iben & Tutukov (1984) and Nelemans & Tauris (1998), based on results of Mengel et al (1979)

$$\dot{M}_c = 10^{-5.36} \left( \frac{M_c}{M_\odot} \right)^{6.6} M_\odot \text{ yr}^{-1}. \quad (9)$$

The RGB stellar radius is calculated according to the relation proposed by Iben & Tutkov (1984)

$$R_g = 10^{3.5} \left( \frac{M_c}{M_\odot} \right)^4 R_\odot \quad (10)$$

The rate of angular momentum carried by the wind (defined positively) in a synchronized system (primary rotation synchronized with orbital motion) is given by (Soker 2002)

$$\dot{J}_{\text{wind}} = \left[ \left( \frac{M_2}{M_g + M_2} \right)^2 a^2 + \beta R_g^2 \right] \omega (-\dot{M}_g). \quad (11)$$

The first term is the angular momentum due to the orbital motion of the primary around the system’s center of mass, while the second term is due to the rotation (spin) of the primary. Here  $-\dot{M}_g = \dot{M}_w > 0$  is the mass loss rate in the wind. We neglect accretion by the secondary. The rate of change in the orbital angular momentum  $J_{\text{orb}} = \mu(GMa)^{1/2}$ , where  $\mu = M_g M_2 / M$  is the reduced mass, and  $M = M_g + M_2$  is the total mass of the binary system, is given by

$$\frac{\dot{J}_{\text{orb}}}{J_{\text{orb}}} = \frac{\dot{M}_g}{M_g} - 0.5 \frac{\dot{M}_g}{M_g + M_2} + 0.5 \frac{\dot{a}}{a}. \quad (12)$$

The rate of change of the envelope angular momentum  $J_{\text{env}} = I_{\text{env}} \omega$  is  $\dot{J}_{\text{env}} = \dot{I}_{\text{env}} \omega + \dot{\omega} I_{\text{env}}$ . Substituting  $I_{\text{env}} = \eta M_{\text{env}} R_g^2$ , the synchronization condition  $\omega = \sqrt{G(M_g + M_2)/a^3}$ , and assuming that  $\eta$  does not vary along the RGB, gives after some rearrangement

$$\frac{\dot{J}_{\text{env}}}{J_{\text{env}}} = \frac{\dot{M}_{\text{env}}}{M_{\text{env}}} + 2 \frac{\dot{R}_g}{R_g} + 0.5 \frac{\dot{M}_g}{M_g + M_2} - 1.5 \frac{\dot{a}}{a}. \quad (13)$$



Substituting Eqs. 11- 13 into Eq. 4 gives ( $M = M_g + M_2$ ):

$$\begin{aligned} \frac{\dot{a}}{a} \left[ 1 - 3\eta M_{\text{env}} \frac{M}{M_g M_2} \left( \frac{R_g}{a} \right)^2 \right] = & -\frac{\dot{M}_g}{M} \left[ 1 - 2\beta \frac{M^2}{M_g M_2} \left( \frac{R_g}{a} \right)^2 \right] \\ -2\eta \frac{\dot{M}_{\text{env}} M}{M_g M_2} \left( \frac{R_g}{a} \right)^2 - \eta \frac{M_{\text{env}} \dot{M}_g}{M_g M_2} \left( \frac{R_g}{a} \right)^2 - & 4\eta M_{\text{env}} \frac{\dot{R}_g}{R_g} \frac{M}{M_g M_2} \left( \frac{R_g}{a} \right)^2. \end{aligned} \quad (14)$$

### 3.2. Solution procedure

The solution was obtained under the following assumptions and performing the following steps.

- (1) We chose initial conditions: Core mass  $M_c$ . This fixed the RGB radius by equation (10). RGB stellar mass  $M_g$ ; companion mass  $M_2$ ; orbital separation  $a$  with a circular orbit; coefficient  $\eta_R$  of the mass loss formula (8). For the RGB envelope's moment of inertia we take  $\eta = 0.2$ , and for the angular momentum loss we take  $\beta = 2/3$  in equation (11), as appropriate for a uniform (spherical) mass loss geometry from the surface of the RGB star.
- (2) The tidal interaction depends very strongly on the ratio of the stellar radius to orbital separation ( $R_g/a$ ). We therefore assume, as in section 2, that tidal interaction is negligible, until the RGB stellar radius is large enough, when a strong tidal interaction occurs. We take this ratio to be  $R_g = 0.2a$ .
- (3) As in section 2, the onset of the tidal interaction results in one of three possibilities. (i) The orbital angular momentum is too low, and no synchronization is achieved. The companion spirals-in to the RGB envelope. (ii) Synchronization between the orbital motion and the RGB rotation is reached, but the system at that stage is unstable to the Darwin instability (see eq. 5). Here again, the companion spirals-in within a very short time to form a CE. (iii) Synchronization is achieved and the system is stable. This evolutionary rout is further evolved, as described below.
- (4) After synchronization is achieved in a stable system, we start to evolve the primary star. The growth of the core mass is according to the rate of hydrogen nuclear burning that forms helium, as given in equation (9). This mass is removed from the envelope. It changes the moment of inertia of the envelope, but not its angular momentum.
- (5) Simultaneously with the growths of the core we consider the wind, by removing mass and angular momentum from the RGB star, according to equations (8) and (11), respectively.
- (6) As the wind carries angular momentum, and the growth of the core changes the RGB moment of inertia, in each time steps we solve equation (14) to determine a new orbital separation  $a$ .
- (7) In each time step we check whether one of the following occurs. (i) The RGB envelope has been completely depleted. We register the orbital separation. (ii) The RGB core has reached a mass of  $M_c = 0.48M_\odot$ , when a core helium flash is assumed to occur. We register the orbital separation. (iii) The Darwin instability occurs. In this case a late CE is formed. We register the RGB envelope rotation velocity. (iv) The increasing radius of the RGB reached the orbital separation  $R_g = a$ . In this case a late CE occurs.

### 3.3. Results

#### 3.3.1. Evolution of orbital separation and envelope mass

We solved for the evolution according to the steps outlined in section 3.2. In Figs. 3 and 4 we present the outcome of the evolution for our two mass loss rates:  $\eta_R = 3 \times 10^{-14}$  (normal) and  $\eta_R = 3 \times 10^{-13}$  (high), respectively, in equation (8). In these sets of calculations the initial core mass is  $M_c(0) = 0.4M_\odot$ , such that the RGB radius is  $R_{g0} = 81R_\odot$ . As strong tidal interaction starts when  $a = 5R_g$  by our standard parameterizations, so that the initial binary separation is  $a = 405R_\odot$ .

For the normal mass loss rate (Fig. 3) the envelope mass decreases slowly, and so does its moment of inertia. As the RGB radius increases, the Darwin instability sets in and the companion spirals-in to the RGB envelope to form a CE. The CE outcome covers a large area in the  $M_2 - M_g$  plane. It is interesting to compare this case to the case where the RGB evolution is not considered (Fig. 2; Soker 2002). When the increase in core mass and radius are not considered, only a small parameters-area in the  $M_2 - M_g$  plane leads to the formation of a CE phase after a stable synchronization has been achieved. When the increase in radius is taken into account, this area is much larger. For a small area in the  $M_2 - M_g$  plane (lower right) the core reaches a mass of  $M_c = 0.48M_\odot$ , for which a core helium flash is assumed to occur (turning the star to a horizontal branch star), and the binary system does not enter a CE phase. Only much later during the AGB phase the system might enter a CE phase.

For the high mass loss rate (Fig. 4) the envelope mass decreases more rapidly, and so does its moment of inertia. This makes the Darwin instability less likely. For that, in some cases the RGB radius reaches the orbital separation before a Darwin instability occurs. Also, the higher mass loss rate leads to the depletion of the envelope before a Darwin instability occurs in some cases. In addition, mass loss acts to increase the orbital separation. Therefore, for a larger range of parameters-area in the  $M_2 - M_g$  plane (lower right corner) the system does not enter a common envelope at all. Still, binaries that located in a large area in the  $M_2 - M_g$  plane do enter a CE phase after a stable synchronization has been achieved. For these systems the RGB envelope mass decreases, in some cases substantially, before a CE phase sets in.

In Fig. 5 we present the evolution of the scaled orbital separation,  $a/a_0$ , with time, for the two values of the mass loss rate, and for several RGB initial masses. In all runs  $a_0 = 405R_\odot$  and  $M_2 = 0.2M_\odot$ , and all cases that are shown reach a stable synchronized orbit after the initial tidal interaction. The following characteristic of the evolution should be noted.

- (1) The values of  $a/a_0$  start with values of  $a/a_0 < 1$ , because we assume that the initial strong tidal interaction brings the system to synchronization in a short time.
- (2) Since we start the calculation when the RGB is highly evolved (a core mass of  $M_c(0) = 0.4M_\odot$  and a radius of  $R_{g0} = 81R_\odot$ ), the evolution to the end of the RGB is relatively short,  $\lesssim 4 \times 10^6$  yr. If the initial orbital separation is smaller, then strong tidal interaction occurs earlier, when the

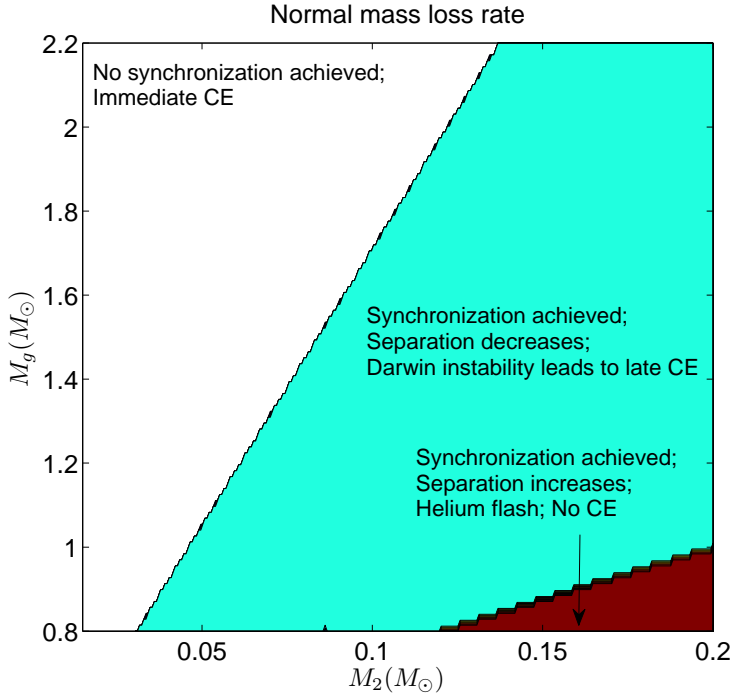


Fig. 3.—  $M_g$  vs.  $M_2$  representing binary systems that reached or did not reach synchronization. Our normal mass loss rate of  $\eta_R = 3 \times 10^{-14}$  was used. The initial core mass is  $M_c(0) = 0.4M_\odot$ , and the initial (primordial) orbital separation prior to tidal interaction is  $a_0 = 5R_g(0) = 405R_\odot$ . Calculation is terminated as indicated, when one of the following occurs. (1) The Darwin instability brings the system to a CE phase (marked ‘Darwin Instability’); (2) The RGB stellar radius exceeds the orbital separation ( $R_g = a$ ; does not happen in this case); (3) A total depletion of the RGB envelope occurs ( $M_{\text{env}}$ ; does not occur in this case due to a relatively low mass loss rate as indicated by  $\eta_R$ ). (4) The core mass reaches  $0.48M_\odot$  and assumed to go through a core Helium flash (‘Helium flash’).

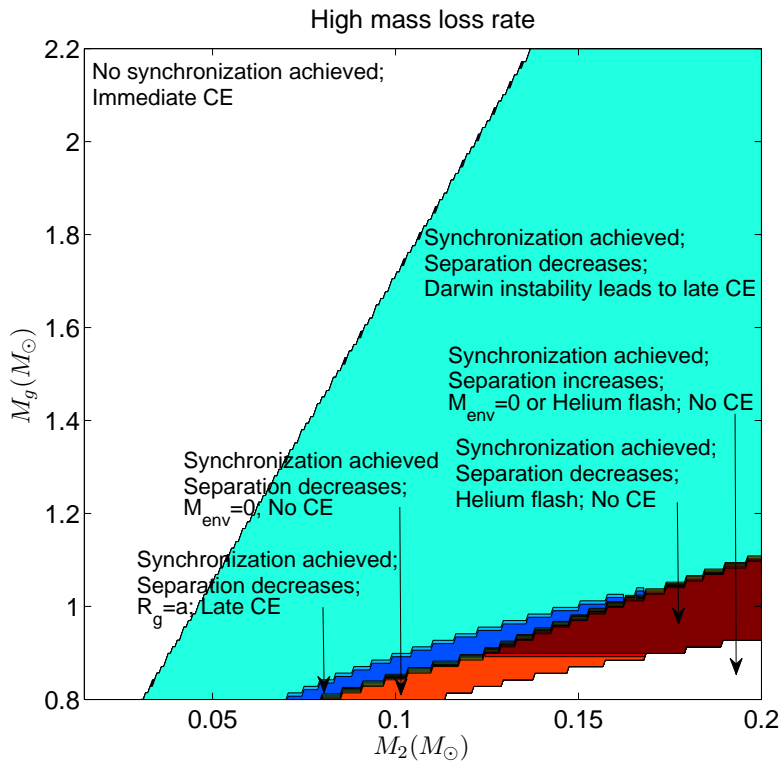


Fig. 4.— Like Fig. 3, but for a high mass loss rate with  $\eta_R = 3 \cdot 10^{-13}$ .

evolution is slower, and the evolution time will be longer.

(3) Synchronization implies that the RGB star rotates at about  $\gtrsim 0.1$  times its break-up speed. Namely,  $\Omega_g \gtrsim 0.1$ . With its strong envelope convection, the synchronized RGB star is likely to have strong magnetic activity. The rotation and magnetic activity are likely to substantially enhance the mass loss rate. For that, we take the high mass loss rate cases to represent our expectation for the mass loss rate.

(4) As expected, a higher mass loss rate reduces the chances for the formation of a CE. Still, by Fig. 4, for a large parameters-area a CE will occur after a substantial mass of the envelope has been lost. The decreases of the envelope mass with time until the onset of a CE phase is presented in Fig. 6. The envelope mass is scaled with its value at the beginning of our calculation (when the system reaches synchronization for the first time).

### 3.3.2. Envelope rotation

We saw that many systems form a CE phase only after the envelope mass has been substantially reduced. Another important effect in all the evolutionary routes considered here is the spinning-up of the RGB envelope before the CE phase starts even. With their strong convection, RGB stars that rotate even at a moderate rate can have a relatively very high mass loss rate.

The envelope angular velocity  $\omega_g$  should be compared with the break up velocity (the velocity of a test body performing a circular Keplerian orbit on the stellar equator)

$$\omega_B \equiv \sqrt{\frac{GM_g}{R_g^3}}. \quad (15)$$

Namely, the important quantity is the ratio  $\Omega_g \equiv \omega_g/\omega_B$ .

The orbital velocity of the RGB envelope  $\omega_g$  changes during the evolution. We will consider four points in the possible evolutionary routes:  $\Omega_{g0}$  : for systems that did not reach a stable synchronized orbit, this is the angular velocity of the envelope when the secondary just enters the envelope;  $\Omega_{g1}$  : when stable synchronization is first achieved;  $\Omega_{g2}$  : when a system with a stable synchronized orbit encounters the Darwin instability and loses synchronization;  $\Omega_{g3}$ ; the primary angular velocity when a system that suffers a Darwin instability just enters the CE phase.

In the first time that tidal interaction takes place, either a stable synchronization occurs or the companion rapidly enters a CE phase. In the case where no stable synchronization occurs, we find that when the companion just enters the RGB envelope the envelope angular velocity is

$$\Omega_{g0} = \frac{\omega_g}{\omega_B} = \frac{\mu}{\eta M_{\text{env}}} \sqrt{\frac{M_g + M_2}{M_g}} \left( \sqrt{\frac{a_0}{R_{g0}}} - 1 \right) \simeq 6 \frac{M_2}{M_{\text{env}}}, \quad \text{no synchronization}, \quad (16)$$

where  $\mu = M_g M_2 / (M_g + M_2)$  is the reduced mass, and where in the last equality we have substituted our standard values of  $\eta = 0.2$ ,  $a_0 = 5R_g$ , and took  $M_2 \ll M_g$ . We can substitute  $M_{\text{env}} =$

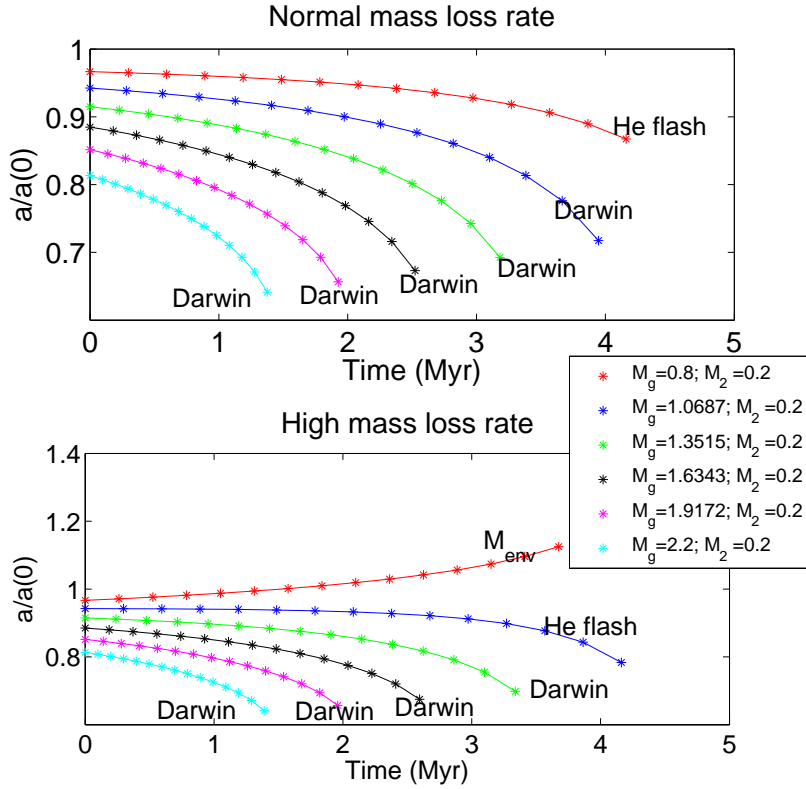


Fig. 5.— Evolution of orbital separation in units of initial orbital separation  $a_0 = 5R_g(0) = 405R_\odot$ , from the moment synchronization is achieved until end of calculation, as explained in the caption of Fig. 3. Top panel is for the normal mass loss rate with  $\eta_R = 3 \times 10^{-14}$  in equation (8), and the bottom panel is for the high mass loss rate with  $\eta_R = 3 \times 10^{-13}$ . The initial mass of the RGB star is indicated for each run. All calculations use a companion mass of  $M_2 = 0.2M_\odot$ , and the RGB core mass at the beginning of the calculation is as in the other runs in this section.

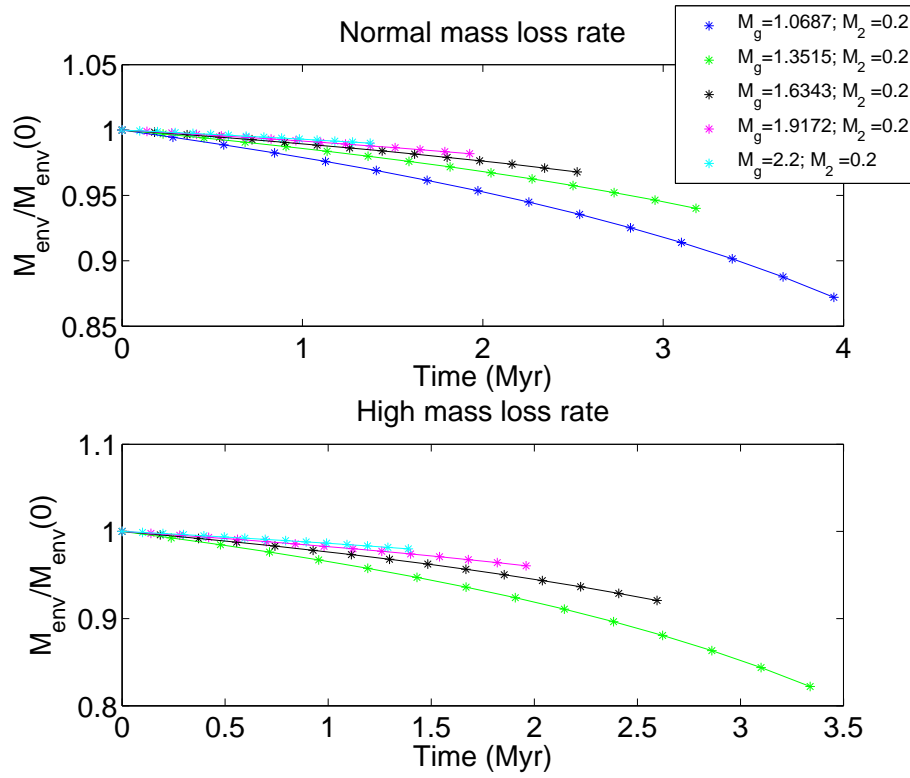


Fig. 6.— Evolution of the envelope mass for the cases presented in Fig. 5 that enter the CE phase. The envelope mass  $M_{env}$  is scaled to its initial value at the moment of synchronization  $M_{env}(0)$ .

$M_{g0} - 0.4M_{\odot}$ , and recast equation (16) in the form

$$M_{g0} \simeq 6 \frac{M_2}{\Omega_{g0}} + 0.4M_{\odot}, \quad \text{no synchronization.} \quad (17)$$

This is a straight line in the  $M_2 - M_g$  plane, as evident in Fig. 7, where we present the values of  $\Omega_{g0}$  when the companion enters the envelope for systems that did not reach stable synchronization. It is evident from Fig. 7 that even when the companion spirals-in very rapidly to the RGB envelope, it manages to spin-up the primary to high rotation velocity. Such rotation speeds are expected to enhance the mass loss rate, even before considering the gravitational energy that is released by the secondary as it spirals-in inside the envelope.

Consider systems that do reach stable synchronized orbit. The scaled envelope’s angular velocity when synchronization is first achieved,  $\Omega_{g1}$ , for these systems is presented in Fig. 8. The condition to achieve a stable synchronized orbit is given in equation (7). (In eq. 7 the assumption  $M_2 \ll M_g$  was used, while in the numerical solutions presented here the exact equations are used; differences are very small). When such a stable synchronized orbit is achieved, the envelope angular velocity, by definition, is equal that of the orbital angular velocity as given by Eq.(3). It is evident that when synchronization is achieved the primary rotates quite rapidly, and strong magnetic activity and enhanced mass loss rate are expected. Note that more massive secondaries bring the RGB envelope to synchronization when they are at larger orbital separations, and hence these systems have lower values of  $\Omega_{g1}$ .

As can be seen in Fig. 4, most binary systems that have a stable synchronized orbit encounter the Darwin instability, and the secondary rapidly spirals-in to form a CE. The normalized RGB angular velocity at the moment the system encounters the Darwin instability,  $\Omega_{g2}$ , is presented in the top panel of Fig. 9. The orbital separation at that moment is presented in Fig. 10. As the secondary rapidly spirals-in during the instability mode, it transfers orbital angular momentum to the envelope, further spinning it up. The normalized RGB angular velocity at the moment the secondary of such a system enters the envelope,  $\Omega_{g3}$ , is presented in the bottom panel of Fig. 9. Fig. 9 shows that the primary can reach very high angular velocity prior to the formation of the CE, and further strengthens our point that the pre-CE evolution must be considered.

It should be noted that although the end result of the systems presented in Fig. 7 and in Fig. 9 is the formation of a common envelope, there is a fundamental difference between these two evolutionary routes. The systems presented in Fig. 7 form a CE shortly after a strong tidal interaction takes place, while those presented in Fig. 9 had evolved through a stable synchronized orbit phase. During that phase the RGB star can lose a substantial fraction of its envelope.



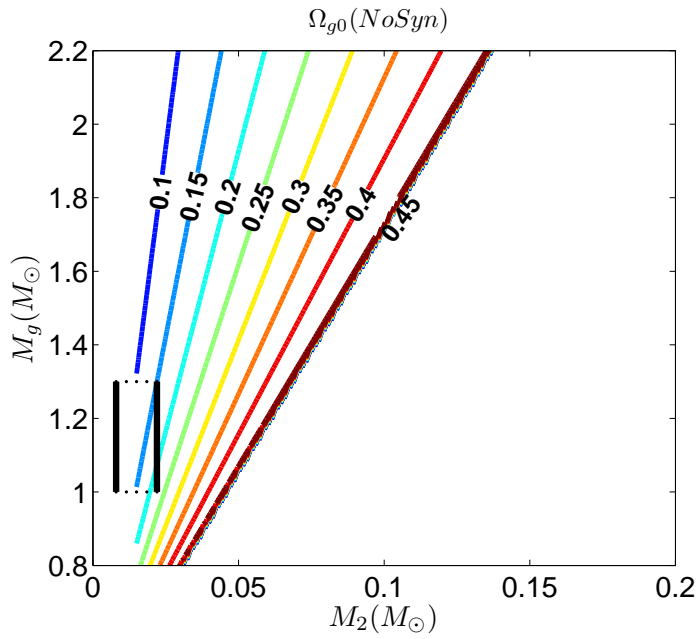


Fig. 7.— The envelope angular velocity scaled by the break up velocity when the companion enters the envelope ( $\Omega_{g0}$ ). The systems presented here did not achieve stable synchronized orbit at all, and therefore the secondary spiralled in directly into the RGB envelope. The black rectangle enclosed the possible area occupied by the progenitor of HD149382 as we discussed in section 4.

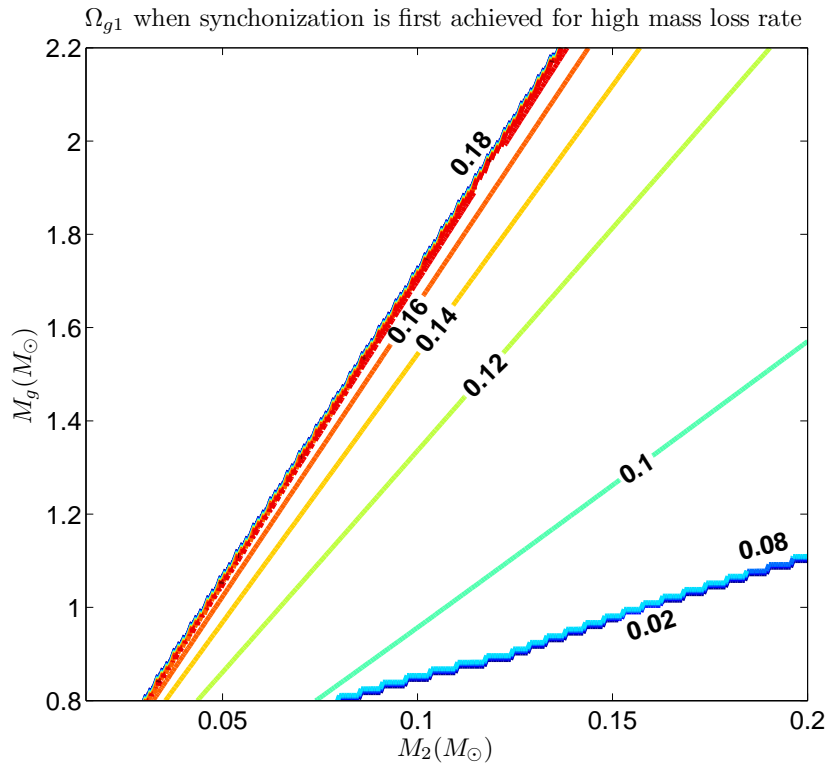


Fig. 8.— The envelope angular velocity scaled by the break up velocity when stable synchronization is first achieved ( $\Omega_{g1}$ ). This figure has the same parameters as Fig. 4, but here only systems that reach synchronization and form a CE later in the evolution are shown. The mass loss parameter has  $\eta_R = 3 \times 10^{-13}$  in equation (8).

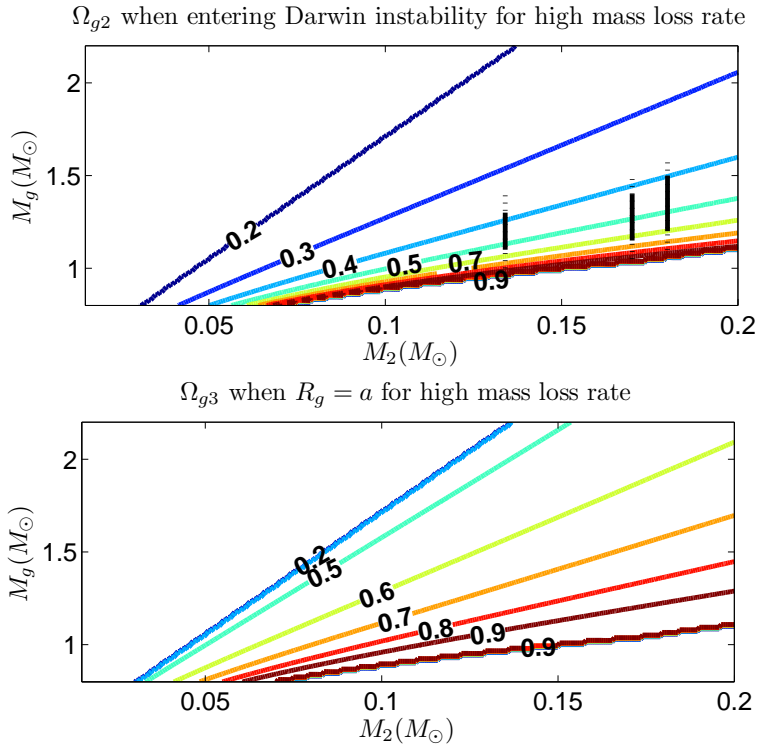


Fig. 9.— The envelope angular velocity scaled by the break up velocity. Top panel represents the envelope angular velocity when the Darwin instability occurs ( $\Omega_{g2}$ ). Bottom panel represents the envelope’s angular velocity when the secondary enters the envelope ( $\Omega_{g3}$ ). The three vertical lines represent the possible locations of the progenitors of the three systems discussed in section 4.

## 4. SUMMARY

We have shown that for a large parameters space binary systems reach stable synchronized orbit before the onset of a common envelope (CE) phase. Although we have made the calculations for RGB stars when their core mass at the beginning of the calculation is  $M_c(0) = 0.4M_\odot$ , the results have wider implications. Such stable orbits can be achieved for other evolved stars, like AGB stars, and for evolutionary stages earlier or later than those used here. Such stable orbits allow the RGB (or AGB, or other evolved giant stars) to lose mass before the onset of the CE. Even after the secondary enters the giant envelope, the rotation velocity is high enough to cause enhanced mass loss rate.

Our results imply that in many cases, studies that neglect the pre-CE evolution (and start with a secondary on the surface of a non-rotating giant) might reach some wrong conclusions. For example, they might conclude that there is a need for extra energy source to expel the envelope, because they do not consider the mass loss process prior to the onset of the CE phase.

Our results can be applied to specific systems. We consider here four systems of sdB stars with companions: HW Vir with  $(M_1, M_2, a) = (0.54M_\odot, 0.18M_\odot, 0.89R_\odot)$  (Wood et al. 1993); PG 1336-018 with  $(M_1, M_2, a) = (0.50M_\odot, 0.17M_\odot, 0.79R_\odot)$  (Kilkenny et al. 1998); HS 0705+6700 with  $(M_1, M_2, a) = (0.483M_\odot, 0.134M_\odot, 0.81R_\odot)$  (Drechsel et al. 2001); and HD149382 (Geier et al. 2009) with  $(M_1, M_2, a) = (0.29 - 0.53M_\odot, 0.008 - 0.022M_\odot, 5 - 6.1R_\odot)$

We mark the possible locations of the progenitors of the first three systems on Fig. 9. The initial mass of the primary is not well constraint, but these systems most probably went through a phase of a stable synchronized orbit. Mass loss rate could have been high, and a non-negligible amount of the RGB envelope has been expelled before the formation of a CE. This increases the survivability of the secondary. If a CE was formed only after the RGB envelope expanded, this can explain the observations that the core was massive enough to experience a core helium flash after the onset of the CE.

The possible location of the progenitor of HD149382 in the  $M_g - M_2$  plane is marked on Fig. 7. This system did not reach synchronization, and a CE phase was formed immediately after a strong tidal interaction occurred. However, the companion did substantially spun-up the envelope, by that increased the mass loss rate. This reduced the envelope mass, and by that increased the survival probability of the companion.

This research was supported by the Asher Fund for Space Research at the Technion, and the Israel Science foundation. E.B. was supported in part by the Minister of Immigrant Absorption.

## REFERENCES

- Alexander M. E., 1976, *ApSS*, 45, 105
- Beer M. E., Dray L., M. King, A. R. & Wynn G. A. 2007, *MNRAS*, 375, 1000
- Catelan, M., 2000, *ApJ*, 531, 826
- Catelan, M., 2009, *ApSS*, 320, 261.(astro-ph/0507464v2)
- Davis P.J., Kolb U., & Willems B., *MNRAS*, ,2009, (arXiv:0903.4152V1)
- D’Cruz N.L., Dorman B, Rood R. T. & O’Connell R. W. 1996, *ApJ*, 466, 359
- D’Cruz N.L., O’Connell, R. W., Rood, R. T., Whitney, J.H., Dorman B, Landsman, W. B., Hill, R. S., Stecher, T. P. & Bohlin R.C. 2000. *ApJ*, 530, 532(arXiv:astro-ph/9909371v1).
- Dewi J.D.M & Tauris T.M.,2000, *A&A*, 360, 1043
- De Marco, O., Sandquist, E. L., Mac Low, M.-M., Herwig, F., & Taam, R. E. 2003, in *The Eight Texas-Mexico Conference on Astrophysics*, Eds. M. Reyes-Ruiz & E. Vazquez-Semadeni, *RMxAC (Serie de Conferencias)*, 18, 24
- Drechsel H., Heber U., Napiwotzki R., Ostensen R., Shlheim J.-E., Johannessen F., Schuh S. L., Deetjen J. & Zola S., 2001, *A&A*. 379, 893
- Geier, S., Edelmann, H., Heber, U., & Morales-Rueda, L. 2009, *ApJ*, 702, L96
- Han Z. 2008, *A&A*, 484, L31.
- Han, Z., Podsiadlowski, Ph., & Lynas-Gray, A. E. 2007, *MNRAS*, 380, 1098
- Han, Z., Podsiadlowski, Ph., Maxted, P. F. L., & Marsh, T. R. 2003, *MNRAS*, 341, 669.
- Han, Z., Podsiadlowski, Ph., Maxted, P. F. L., Marsh, T. R., & Ivanova, N. 2002, *MNRAS*, 336, 449
- Hu, H., Nelemans, G., Ostensen, R., Aerts, C., Vuckovic, M., & Groot, P. J. 2007, *A&A*, 473, 569
- Iben I. Jr. & Tutukov A.V., 1984, *ApJS*, 54, 335
- Kilkenny, D., ODonoghue, D., Koen, C., & van Wyk, F. 1998, *MNRAS*, 296, 329
- Livio M. & Soker N., 1988, *ApJ*, 329, 764
- Livio M. & Soker N., 2002, 571 L161
- Maxted, P.F.L., Heber, U., Marsh, T.R., & North, R.C. 2001a, *MNRAS*, 326, 1391
- Maxted, P.F.L., Marsh, T.R., & North, R.C. 2001b, 12th European Workshop on White Dwarf stars, 226, 187
- Mengel J. G., Sweigart, A. V., Demarque P. & Gross P. G. 1979, *ApJS*. 40, 733
- Menzies, J. W., & Marang, F. 1986, in “Instrumentation and Research Programmes for Small Telescopes,” Eds., J.B. Hearnshaw and P.L. Cottrell, *IAU Sym.* 118 (D. Reidel, Dordrecht, Holland), 305

- Meszaros Sz., Avrett E. H. & Dupree A. K. 2009, *AJ*, 138, 615
- Nelemans G. & Tauris T. M. 1998, *A&A*, 335, L85
- Nelemans, G. & Tout, C. A. 2005, *MNRAS*, 356, 753
- Paczynski B., 1971, *ARAA*. 9. 183
- Politano, M. & Weiler, K. P. 2007, *ApJ*, 665, 663
- Pustynski & Pustylnik 2006, *ACTA Astronomica*, 56, 83
- Reimers D., 1975, *Mem. Soc. R. Liège* 6 Ser., 8, 369
- Schroder K.P. & Cuntz M. 2005, *A&A*, 630, L73
- Schroder K.P. & Cuntz M. 2007, *A&A*, 465, 593
- Soker N., 1998, *ApJ*, 116, 1308
- Soker N., 2002, *MNRAS*, 336, 1229
- Soker N., 2004, *NewA*, 9, 399 (astro-ph/0311168v1)
- Soker N., 2006, *ApJ*, 645, l57-L60.
- Soker N., Harpaz A & Livio M., 1984, *MNRAS* , 210, 189
- Soker N, & Harpaz A. 2000, *MNRAS*, 317, 861
- Soker N, & Harpaz A. 2007, *ApJ*, 660, 699
- Suzuki T. K. , 2007, arXiv:astro-ph/0608195v51.
- Tauris T. M. & Dewi J. D. M., 2001, *A&A*, 369, 170
- Webbink, R. F. 2008, in *Short-Period Binary Stars: Observations, Analyses, and Results*, Eds. E. F. Milone, D. A. Leahy, and D. W. Hobill, (Springer, Berlin), 352, 233
- Whitney, J. H., Rood R. T., O’Connell R. W., D’Cruz N. L.; Dorman B., Landsman W. B., Bohlin, R. C., Roberts M. S.; Smith A. M.; Stecher T. P. 1998, *ApJ*, 495,284.
- Wood, J. H., Zhang, E.-H., & Robinson, E. L. 1993, *MNRAS*, 261, 103

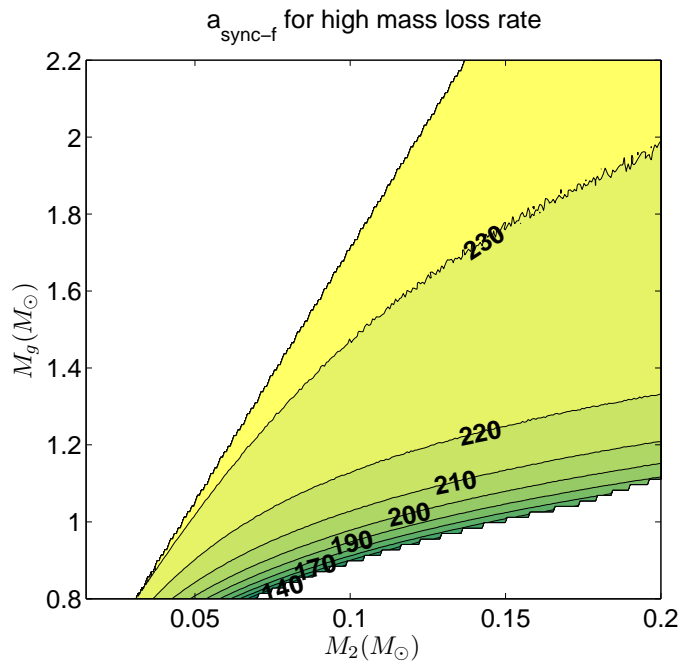


Fig. 10.— Orbital separation when the Darwin instability occurs (and synchronization is lost) for the same systems shown in Fig. 9.